Mean Winds and Momentum Fluxes over Jicamarca, Peru, during June and August 1987

MATTHEW H. HITCHMAN AND KENNETH W. BYWATERS

Department of Atmospheric and Oceanic Sciences, University of Wisconsin—Madison, Madison, Wisconsin

DAVID C. FRITTS

Department of Electrical and Computer Engineering, University of Colorado, Boulder, Colorado

LAWRENCE COY

Department of Earth and Atmospheric Sciences, Saint Louis University, St. Louis, Missouri

ERHAN KUDEKI AND FAHRI SURUCU

Department of Electrical and Computer Engineering, University of Illinois, Champaign, Illinois

(Manuscript received 5 April 1991, in final form 20 February 1992)

ABSTRACT

Data from the mesosphere–stratosphere–troposphere (MST) radar at Jicamarca, Peru, together with other available data, are used to diagnose the mean structure of winds and gravity-wave momentum fluxes from the surface to 90 km during two ten-day campaigns in June and August of 1987.

In the stratosphere a layer of maximum eastward flow associated with the quasi-biennial oscillation (QBO) was seen to strengthen and descend rapidly from June to August, overlying persistent westward flow. A layer of enhanced signal return, suggestive of a turbulent layer, was observed just above the descending QBO eastward maximum. Notable zonal asymmetries were present during this transition and the local meridional circulation departed from zonal-mean QBO theory. A substantial northeastward momentum flux was found below 25 km, which may be related to topographic gravity waves excited by southeastward flow across the Andes.

In the lower mesosphere a relatively weak "second" mesopause semiannual oscillation is confirmed. Gravity-wave zonal and meridional momentum fluxes usually opposed the flow, yielding body forces of $\sim$10–100 m s^{-1} day^{-1}. In both the lower stratosphere and mesosphere, body forces were comparable in magnitude to inferred Coriolis torques.

1. Introduction

The circulation of the tropical middle atmosphere is usually described in terms of phenomena defined by zonal-mean temperature and zonal wind: the annual cycle and time-mean components, the stratospheric quasi-biennial oscillation (QBO), which predominates below $\sim$30-km altitude, the stratopause semiannual oscillation (SSAO), which maximizes near 50-km altitude, and the mesopause semiannual oscillation (MSAO), which maximizes near 80-km altitude (e.g., Hirota 1980; Plumb 1984; Dunkerton and Delisi 1985; Delisi and Dunkerton 1988; Garcia and Clancy 1990). The accompanying meridional circulations have not been measured directly, and little is known about possible zonal variations in these motions. Gravity-wave momentum fluxes are believed to play a significant role in driving these phenomena (Dunkerton 1982; Hamilton and Mahlman 1988; Hitchman and Leovy 1988; Gray and Pyle 1989), but direct estimates in the tropics have not been made before. Mesosphere–stratosphere–troposphere (MST) radars are very sparse geographically and have a signal gap in the layer $\sim$35–65 km, but they have excellent temporal sampling and vertical resolution. They provide the primary means of estimating local gravity-wave momentum fluxes as well as the local background circulation.

Two 10-day campaigns were conducted at the Jicamarca, Peru, MST radar facility during June and August of 1987. A companion paper (Fritts et al. 1992) describes tidal motions, evidence for inertial instability, and the considerable temporal variability of winds and momentum fluxes. Here we describe the time-mean profiles of winds and momentum fluxes for each campaign. Contemporaneous tropical radiosonde and rocketsonde data as well as analyses from the European Centre for Medium-Range Weather Forecasts (ECMWF) were obtained for comparison. These ob-

Corresponding author address: Dr. Matthew H. Hitchman, Department of Atmospheric and Oceanic Sciences, University of Wisconsin, 1225 West Dayton Street, Madison, WI 53706.

servations contribute toward a circulation climatology, capturing the MSAO and QBO at two phases, and provide the first estimates of mean gravity wave momentum fluxes and body forces in the equatorial stratosphere and mesosphere. In section 2 we describe the MST radar data and auxilliary data. Wind profiles are presented in section 3, followed by the gravity wave momentum fluxes and body forces in section 4. Section 5 explores the possible implications of these new observations for the structure of the tropical atmosphere.

2. Methods and analysis

a. Jicamarca MST radar

The wind and momentum flux measurements were taken at the Jicamarca Radio Observatory (12°S, 77°W) during 16–23 June and 4–13 August 1987. The radar was configured to have four independent beams steered 2.5° from the zenith in the geomagnetic north, south, east, and west directions. Line-of-sight mean Doppler velocity estimates were combined to estimate meteorological wind components and momentum fluxes using the procedures described in this section. Further information about the experimental design is given in Fritts et al. (1992) and Bywaters (1990).

The MST radar technique was pioneered by Woodman and Guillen (1974) to infer bulk air velocity from the mean Doppler shift of radiowave signals scattered from refractive index irregularities with a characteristic length scale of one-half the radio wavelength. These irregularities arise from turbulent variations in temperature, humidity, and electron density gradients embedded in the flow. The Jicamarca MST radar emits pulses of electromagnetic radiation at a frequency of 50 MHz, corresponding to a carrier wavelength of 6 m. Discrete power spectra were assembled from returned pulses and processed to give 1-minute radial velocity averages at 500-m vertical resolution. In the troposphere and stratosphere, humidity and temperature fluctuations are largely responsible for refractive index irregularities and useful signal returns can be obtained at Jicamarca at all times in the layer ~20–35 km, with suitable temporal averaging. In the mesosphere, electron fluctuations are most important. Since the free electron concentration decreases rapidly below 60 km and after sunset at all levels, mesospheric observations were obtained only during daylight hours and in the layer ~65–90 km. Above 90 km plasma instabilities become important in controlling the irregularities. Between 35 and 65 km refractive index irregularities are too weak to provide useful velocity estimates.

We calculate the most stable estimates of winds and momentum fluxes by averaging all of the data for each campaign. Since the mesosphere can be sampled only during the day, we restricted observations to daylight hours. Mesospheric signals are typically much weaker than stratospheric signals, so our sampling schedule dedicated the first 5 minutes of each hour to the stratosphere and the last 55 minutes to the mesosphere. Here we report on the average of 1-minute measurements taken during 16–23 June (8 days) and 4–13 August (10 days), for which more than 10 total hours of data are available each day.

The Doppler spectra were parameterized by their zeroth, first, and second central moments. The zeroth moment corresponds to the sum, P, of the total scattered signal, S, and system noise, N. In the results to be presented here, only values with $P/N > 1.47$ (corresponding to -3.25 dB) are included in the analysis. The first moment, or mean Doppler shift of the return signal, is proportional to the mean line-of-sight velocity. Meteor echoes were filtered out by making use of their characteristically broad spectra.

b. Winds and momentum fluxes

In order to calculate momentum fluxes in the north–south and east–west planes, hardware modifications were made for our experiment to compensate for the slightly tilted alluvial plane (Woodman et al. 1989; Fritts et al. 1992). With the array rephased so that the four beams are centered about the zenith, momentum flux estimates in the north–south and east–west planes were then possible. Fritts et al. (1992) computed vertical velocities separately for each beam pair to ascertain vertical pointing precision. Given the limitations of side-lobe interference, each beam was steered only 2.5° from the zenith. The main lobe for each beam has a half-power width of 0.7° in the vertical plane. At 80-km altitude the beam pair centers are 7 km apart and the half-power diameter of each beam is ~1 km. The relatively small ratio of beam separation to beamwidth may contribute to errors in velocity estimates.

Estimates of zonal, meridional, and vertical velocity components were obtained from

$$\bar{u}(z) = \frac{\bar{U}_e(R) - \bar{U}_w(R)}{2\sin\theta} \tag{1a}$$

$$\bar{v}(z) = \frac{\bar{U}_n(R) - \bar{U}_s(R)}{2\sin\theta} \tag{1b}$$

$$\bar{w}(z) = \frac{\bar{U}_e(R) + \bar{U}_w(R) + \bar{U}_n(R) + \bar{U}_s(R)}{4\cos\theta}, \tag{1c}$$

where the subscripts e, w, n, and s correspond to the four radar beams directed toward the east, west, north, and south; θ is the zenith angle; $R = cT/2$ is the target range, where c is the speed of light and T is the sampling delay; $z = R\cos\theta$ is the geometric height; and the overbar indicates the campaign mean of one-minute radial velocities (Vincent and Reid 1983). Since geomagnetic north is 6°01′ east of geographic north, one-minute wind estimates were rotated to obtain $\bar{u}$ and $\bar{v}$ in meteorological coordinates. This transformation made a substantial difference for the relatively smaller meridional wind component.

Vincent and Reid (1983) introduced an appealingly simple method of estimating momentum fluxes due to gravity waves. It is based on the principle that eddy motions in tilted phase planes will give larger line-of-sight velocities along one look direction than along another. The zonal and meridional momentum fluxes per unit mass are estimated from the formulas

$$\overline{uw}(z) = \frac{\overline{U_e^2}(R) - \overline{U_w^2}(R)}{2\sin 2\theta} \tag{2a}$$

$$\overline{vw}(z) = \frac{\overline{U_n^2}(R) - \overline{U_s^2}(R)}{2\sin 2\theta}. \tag{2b}$$

These flux components were rotated to meteorological coordinates, then used to estimate the zonal and meridional body forces per unit mass:

$$DF_u = -\frac{1}{\rho_0}\frac{\partial}{\partial z}(\rho_0 \overline{uw}) \tag{3a}$$

$$DF_v = -\frac{1}{\rho_0}\frac{\partial}{\partial z}(\rho_0 \overline{vw}) \tag{3b}$$

where ρ_0 is the basic-state density (e.g., Andrews et al. 1987). Eddy momentum fluxes were estimated as residuals by subtracting the portion due to the mean circulation from the total: $\rho_0\overline{u'w'} = \rho_0\overline{uw} - \rho_0\bar{u}\bar{w}$, $\rho_0\overline{v'w'} = \rho_0\overline{vw} - \rho_0\bar{v}\bar{w}$.

The estimators (2) and (3) are based on the assumption of statistical homogeneity of the motion field over scales larger than the radar beam separation. Under this assumption, horizontal gradients of eddy correlations over the radar site are zero and the campaign-mean body forces may be used in the local momentum equations to assess how reasonable their magnitudes are:

$$-2\Omega\bar{v}\sin\phi + \frac{\partial\bar{\Phi}}{\partial x} = DF_u \tag{4a}$$

$$2\Omega\bar{u}\sin\phi + \frac{\partial\bar{\Phi}}{\partial y} = DF_v \tag{4b}$$

where the symbols have their usual meaning (e.g., p. 32 of Holton 1975), except $\overline{(\ )}$ indicates a time mean.

c. Auxiliary data

Velocity, momentum flux, and body force estimates may be subject to systematic errors arising from the aspect sensitivity of the scattering process, insufficient or discontinuous time averaging, and fine structuring of enhanced turbulent layers less than 500 m thick, as well as horizontal inhomogeneities in the gravity wave field. Recognizing the possibility of such errors, we have sought as much comparative data as possible. For the June campaign, conventional rawinsonde soundings at Callao, located 30 km west of Jicamarca, and regional surface synoptic charts were provided by Jose and Elio Loja. The six June soundings typically extended from the surface to about 25-km altitude. Barbara Naujokat provided the four Ascension Island (8°S, 56°W) rocket profiles, as well as the monthly mean radiosonde profiles from Singapore (1°N, 104°E). The rocket profiles typically span the layer 20–65 km with 1-km resolution. Kevin Trenberth provided the ECMWF analyses, which include satellite data and are described by Hollingsworth et al. (1986) and Trenberth and Olson (1988).

3. Winds

a. Comparison with auxiliary data

Wind component profiles from radar, rocket, and balloon are plotted in Figs. 1 and 2 for June and August 1987. The vertical range of 0–90 km emphasizes the limitations and strengths of MST radar data coverage. The 20–35-km and 65–90-km layers span 45% of the total depth. The mesospheric layer contributes uniquely, while the stratospheric layer bridges the upper part of rawinsonde profiles and the lower part of rocketsonde profiles. When comparing profiles it should be kept in mind that the mean MST radar and 16 June Callao rawinsonde profiles are near 12°S, 77°W; the two individual rocket profiles from Ascension Island are at 8°S, 14°W; and the monthly mean rawinsonde profiles from Singapore are at 1°N, 104°E.

The tropospheric soundings agree fairly well with climatology for the region (Newell et al. 1974; Oort 1983), except that the winds are much stronger. On 16 and 18 June at Callao an extraordinarily strong poleward flow (~ -25 m s^{-1}) coincided with the upper-tropospheric subtropical eastward jet of ~ 30 m s^{-1} (Fig. 1), consistent with enhanced large-scale outflow from convection to the north (cf. Fig. 3). The tropopause was observed at 16.5 km (100 mb), with a temperature of 196 K on 16 June. Strong and variable flow over topography is implicated by these tropospheric soundings. The Andes reach 6768 m at Huascaran and the flow near 5-km altitude was predominantly from the northeast (Fig. 1).

In the stratosphere during both June and August, zonal wind profiles at widely separated locations were noticeably different (Figs. 1 and 2). The ECMWF analyses at 30 mb ($\sim$23 km in the tropics) in Fig. 4 also exhibited this geographical variation. One might expect such variation in the lowest part of the stratosphere (Newell and Gould-Stewart 1981) but not necessarily at these levels. In addition to substantial meridional shears of zonal wind within the tropics, these analyses show zonal variations of 10–20 m s^{-1}. Near 30 mb during June the zonal flow was ~ -25 m s^{-1} at Singapore, ~ -20 m s^{-1} at Ascension Island, and ~ -15 m s^{-1} at Jicamarca. By August the equatorial flow had become eastward (~ 10 m s^{-1}) in the eastern hemisphere, while it was still westward (~ -10 m s^{-1}) at Ascension Island and Jicamarca.

In the layer 35–55 km a moderate westward trend

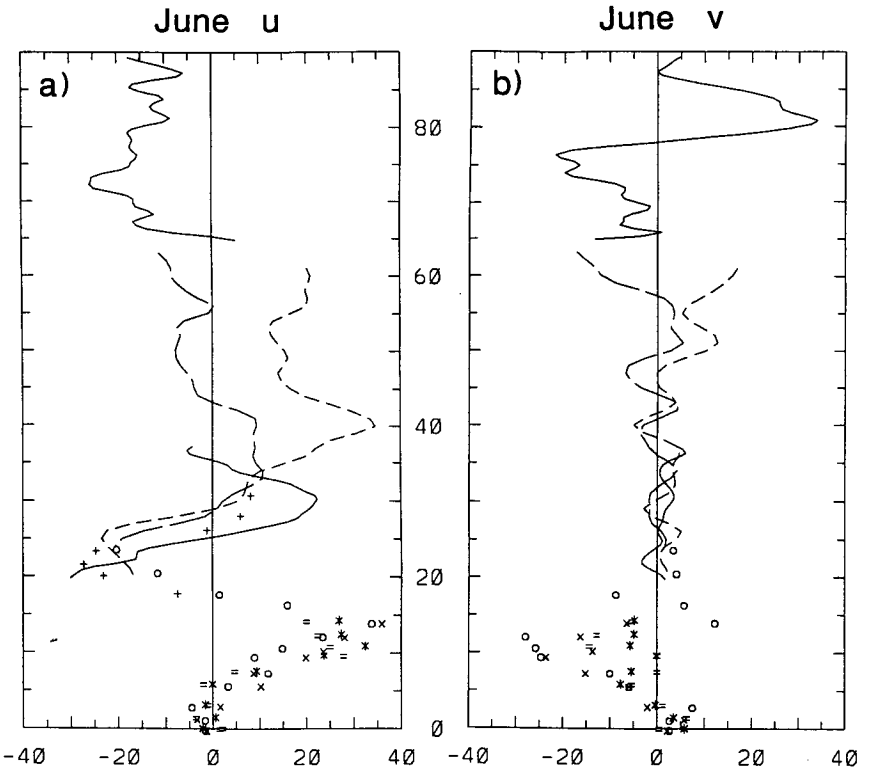

FIG. 1. Profiles of (a) zonal and (b) meridional wind (range ±40 m s^{-1}) for June 1987 in the altitude range 0–90 km. Solid curves are MST radar values at Jicamarca (12°S, 77°W) for the period 16–23 June. Plus signs represent June mean rawinsonde values at Singapore (1°N, 104°E). Rawinsonde soundings at Callao, 30 km west of Jicamarca, are shown for 16 (O), 18 (×), 20 (*), and 22 (=) June. The Ascension Island (8°S, 14°W) rocket profiles are denoted by short dashes (3 June) and long dashes (17 June).

from ~10 m s^{-1} in June to ~ −20 m s^{-1} in August occurred. This agrees with climatology, where the SSAO is expected to be stronger in the "first cycle" (January–June) than in the "second cycle" (July–December) (Hitchman and Leovy 1986; Delisi and Dunkerton 1988). Although meridional winds at Ascension Island and Jicamarca do not agree in detail, this comparison shows that radar meridional winds are not overly large. Detailed agreement is not necessarily expected because the rocket profiles sample an instantaneous wave field, while the radar profile is a time average.

In the mesosphere the match between the rocket and radar wind profiles near 65 km is reasonably good, with rocket profiles exhibiting large temporal variability. An MSAO eastward tendency near 75 km is inferred and the flow was toward the winter hemisphere below 80 km. Large vertical shears in both wind components appeared in June and August.

b. Lower stratosphere

Figure 5 shows the zonal (solid), meridional (short dashed), and vertical (long dashed) Jicamarca wind components for June (left) and August (right) in the stratosphere. In June a deep layer of eastward flow was found between 25 and 35 km, with a maximum speed of 25 m s^{-1} near 31 km. Westward flow maximized at −30 m s^{-1} near 20 km. By August the eastward maximum had strengthened to 35 m s^{-1} and descended to 28.5 km, with westward flow appearing above 32.5 km. The altitude of the lower zero wind line was the same in June and August, although the westward flow below 23 km was substantially weaker by August. Both the upper zero wind line and eastward maximum descended 2.5 km between data midpoints 20 June and 8 August, for a descent rate of 1.5 km mo^{-1}. This is 50% faster than expected from climatology (Naujokat 1986). The Singapore profiles (compare Figs. 1a and 2a) exhibited a descent rate for the lower zero wind line of 2.2 km mo^{-1}, the fastest rate since records began in 1953 (Naujokat, personal communication 1990). It appears that the narrow leading "nose" of eastward flow (Hamilton 1984; Dunkerton and Delisi 1985) arrived at 30 mb first in the eastern hemisphere (Fig. 4). Surprisingly, eastward flow at 50 mb was again restricted to the eastern hemisphere at the end of this QBO phase in early 1989 (Rood et al. 1992).

Previous observational estimates of the meridional

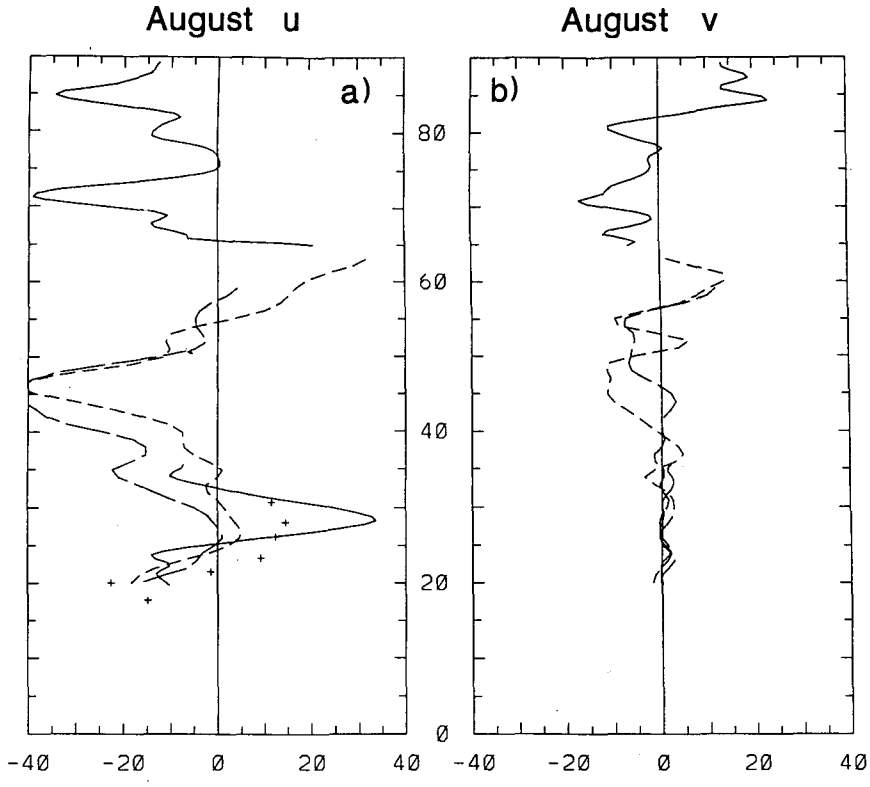

FIG. 2. Profiles of (a) zonal and (b) meridional wind (range ±40 m s^{-1}) for August 1987 in the altitude range 0–90 km. Solid curves are MST radar values at Jicamarca (12°S, 77°W) for the period 3–12 August. Plus signs represent August mean rawinsonde values at Singapore (1°N, 104°E). The Ascension Island (8°S, 14°W) rocket profiles are from 11 August (short dashes) and 20 August (long dashes).

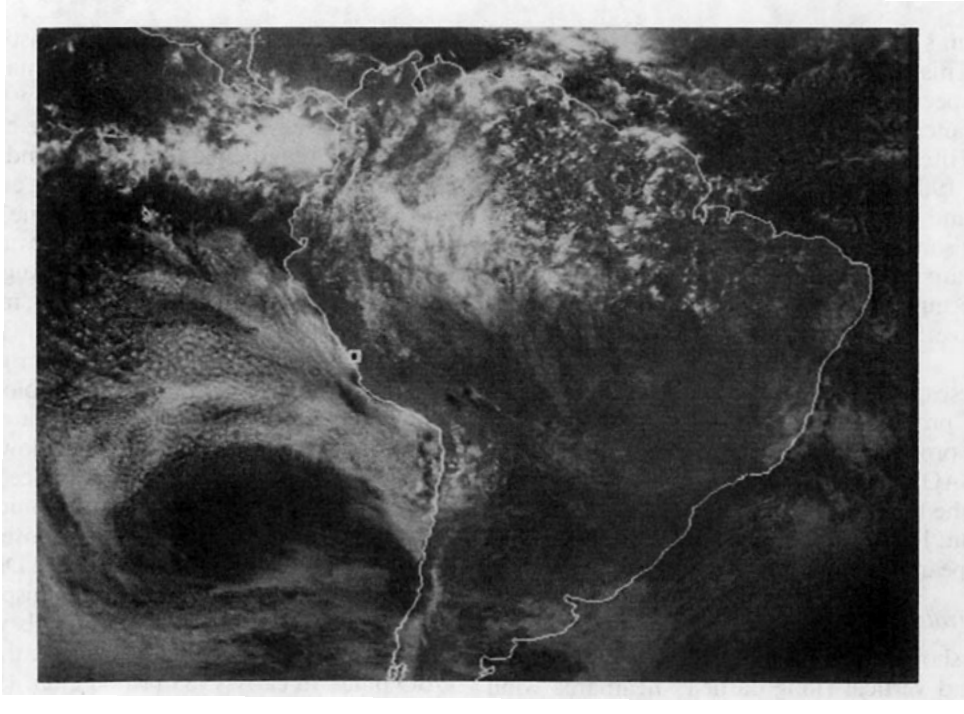

FIG. 3. GOES-East visible image on 20 June 1987.

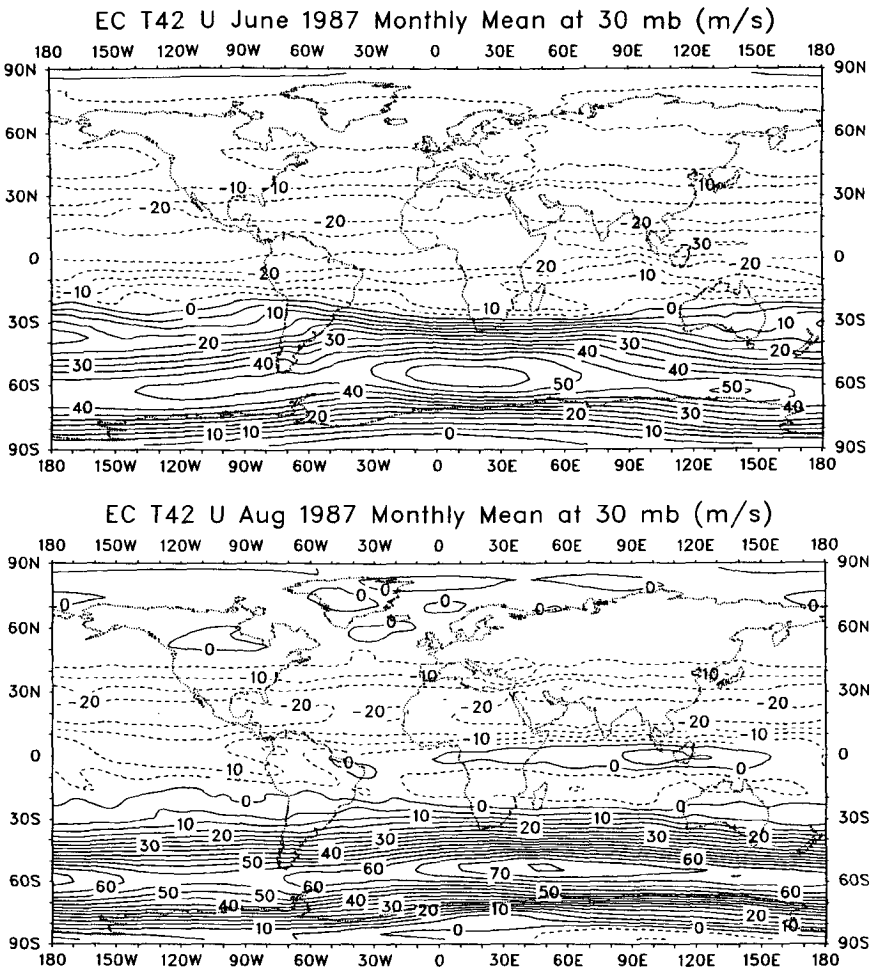

FIG. 4. ECMWF analyses of monthly mean 30-mb zonal wind for (a) June and (b) August 1987, contour interval 5 m s^{-1}, courtesy of Kevin Trenberth and Amy Solomon.

circulation in the tropical stratosphere are lacking, due to sampling problems. Numerical models of the zonal-mean QBO suggest very small amplitudes (Plumb and Bell 1982; Dunkerton 1985; Gray and Pyle 1989; Dunkerton 1991). For a zonal wind amplitude of 20 m s^{-1} and temperature perturbation of 1.5 K, the largest theoretical meridional and vertical speeds are $\sim$0.05 m s^{-1} and $\sim 5 \times 10^{-5}$ m s^{-1}. At 12°S eastward winds should be accompanied by northward flow and westward winds by southward flow. This expectation is supported by satellite estimates of the distributions of aerosol and potential vorticity, which also suggest enhanced lofting near 12°S when there is eastward shear over the equator (Trepte and Hitchman 1992).

In June the descending QBO layer of eastward flow was accompanied by northward flow reaching $\sim$3 m s^{-1}, while the westward flow was accompanied by southward flow reaching ~ -3 m s^{-1}. In August the meridional flow was weaker with no apparent relationship to the zonal flow. Vertical motions were downward in QBO eastward flow, with a maximum of ~ -10 cm s^{-1}. Vertical motions were weaker in the westward flow. Compared to expectations from the zonal-mean theory of the QBO, observed local meridional circulations were much stronger and did not have the same spatial relationship with the zonal flow. Although it is quite possible that standing topographic gravity waves contributed to these profiles, stratospheric vertical motions were larger than expected from diabatic considerations and their interpretation remains uncertain.

Profiles of signal-to-noise ratio for the east–west beam pair for June (solid) and August (dashed) are shown in Fig. 6. Values were typically 25 dB at altitudes below 25 km, falling exponentially to less than zero above 34 km. An extraordinary secondary maximum was found near 33-km altitude in June, which descended to 30.5 km by August. This secondary maximum of power enhancement by $\sim$5 dB lay 2 km above the eastward flow maximum and both descend monotonically in daily mean profiles (not shown). This unexpected layer of enhanced signal return was probably

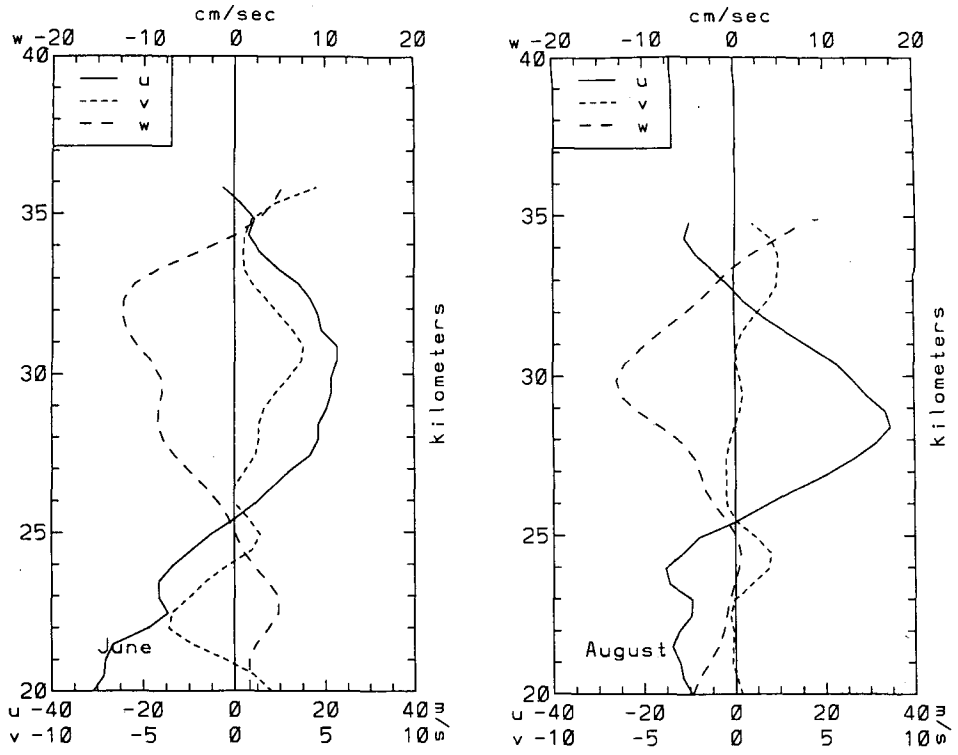

FIG. 5. Stratospheric radar profiles of zonal (solid, range ±40 m s^{-1}), meridional (short dashed, range ±10 m s^{-1}), and vertical (long dashed, range ±20 cm s^{-1}) wind component averaged for the June (left) and August (right) 1987 Jicamarca campaigns.

due to increased turbulence. One may speculate that this was caused by westward-propagating gravity waves breaking in westward shear.

c. *Mesosphere*

Wind components in the mesosphere for June and August are shown in Fig. 7. In June zonal winds were in the range −7 to −25 m s^{-1} throughout the layer 70–85 km. By August winds near 75 km were ~0 m s^{-1}, while the westward flow near 72 km had strengthened to ~ −35 m s^{-1}. The general westward character and eastward vertical shear of these profiles agrees well with Hirota's (1978) results for 1971 at Ascension Island (8°S, 56°W) and with Hamilton's (1982) results for the period 1969–75 at Kwajalein (9°N, 168°E), where special high-altitude rockets were employed. Hamilton found a weakening of westward flow above 70 km from June to August. Garcia and Clancy (1990) studied mesospheric temperature data derived from the Solar Mesosphere Explorer instrument. They found that the MSAO during the period 1982–86 was quite variable from year to year. Nevertheless, in the 70–75-km layer a warm anomaly usually arrived between June and August, which is compatible with the enhanced eastward shear in that layer seen in the radar data in August compared to June. Their data also showed a weak "second cycle" of the MSAO near 70 km, which can be accounted for by a weak "second cycle" of the underlying SSAO and filtering of gravity waves (Dunkerton 1982).

Two recent radar studies confirm this picture of descending eastward shear that is robust in some years but not in others. Radar observations of tropical mesospheric flow were obtained at Christmas Island (2°N, 158°W) during August and September of 1988 by Avery et al. (1989), who used meteor echoes to infer zonal and meridional winds in the layer 82–98 km. In the overlap region 82–85 km, they also found westward monthly mean winds, but with magnitudes less than 10 m s^{-1}. Vincent and Lesicar (1991) reported observations of mesospheric winds during January–August 1990 with an MF partial reflection radar, also at Christmas Island. In June near 75 km the flow turned from ~ −10 m s^{-1} in June to ~10 m s^{-1} in August.

The diabatic cross-equatorial flow toward the winter hemisphere near solstice derived in numerical models (e.g., Wehrbein and Leovy 1982; Hitchman et al. 1989) and from LIMS data (Kiehl et al. 1986; Gille and Lyjak 1986; Hitchman and Leovy 1986) predict flow toward the winter hemisphere of perhaps 5–10 m s^{-1} peaking near 60 km and increasing again above ~70 km. In agreement with theoretical expectations from seasonal global overturning, the June meridional flow below 78 km is southward, reaching −15 to −20 m s^{-1} near 75 km. In contrast, above 81 km northward flow predom-

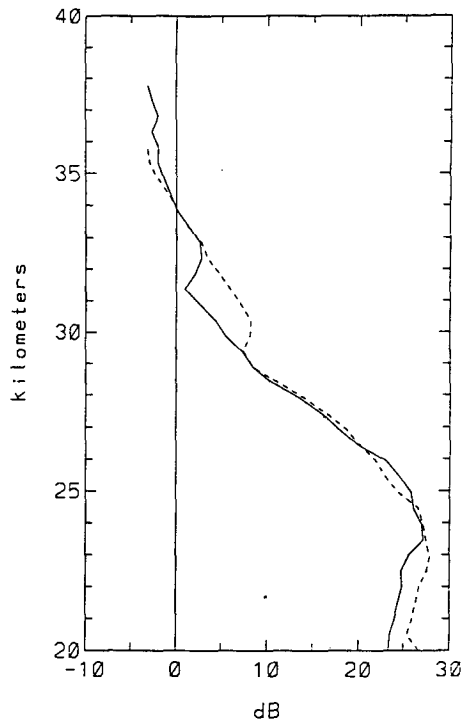

FIG. 6. Stratospheric profiles of signal-to-noise ratio for the June (solid) and August (dashed) campaigns, range −10 to 30 dB.

inates, reaching 35 m s^{-1}. Below 75 km in August flow has weakened at all levels. This behavior is similar to the results of Vincent and Lesicar (1991) for June and August 1990, and is compatible with the northward flow near 82 km for August 1988 found by Avery et al. (1988).

Apparent vertical motions reaching tens of centimeters per second were also found over Jicamarca. Large vertical motions have also been observed with the Poker Flat and SOUSY MST radars near the high-latitude mesopause (Balsley and Riddle 1984; Fritts and Yuan 1989; Fritts and Wang 1990). Several factors may account for the large vertical velocities, including beam-pointing errors and sensing Eulerian rather than Lagrangian motions (Coy et al. 1988). Indeed, wave amplitudes and inferred energy fluxes appear to be as large at Jicamarca as at higher latitudes, implying equally large Stokes drifts. Alternatively, these measurements are much more sensitive to possible beam-pointing errors than those with other systems because of the small off-vertical pointing angles. However, there is no obvious correlation of w with u or v that is common to all observation intervals.

4. Momentum fluxes and body forces

Perhaps the chief contribution that MST radars can make toward understanding the general circulation and

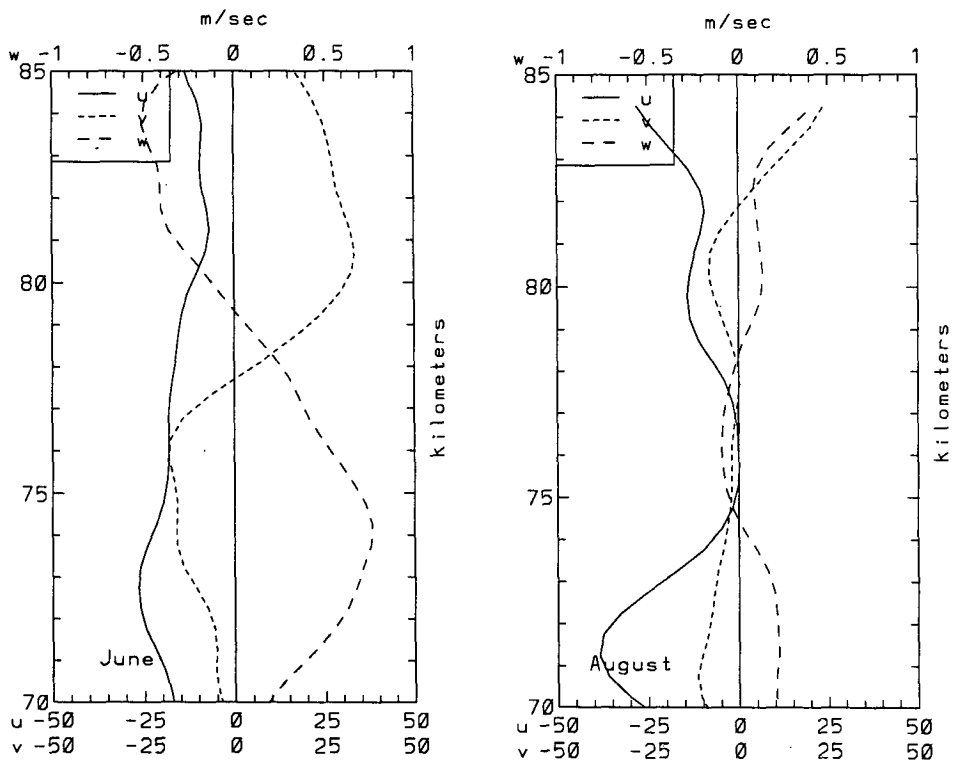

FIG. 7. Mesospheric radar profiles of zonal (solid, range ±50 m s^{-1}), meridional (short dashed, range ±50 m s^{-1}), and vertical (long dashed, range ±1 m s^{-1}) wind components averaged for the June (left) and August (right) 1987 Jicamarca campaigns.

the role of wave forcing is in estimating momentum fluxes by subplanetary-scale waves that cannot be detected by satellite. The tropical South American region is likely to be a rich source for gravity waves, with substantial flow over topography (Fig. 1) and diverse convective centers. During June and August convection over the Amazon is less than average, but convection in the Gulf of Panama is quite active (Fig. 3).

a. Stratosphere

Figure 8 shows the stratospheric momentum fluxes per unit volume, with the contribution by the mean circulation removed, together with the corresponding body forces per unit mass for June and August in the east–west (left) and north–south (right) planes. In general, $|\rho_0\overline{u'w'}| > |\rho_0\bar{u}\bar{w}|$ and $|\rho_0\overline{v'w'}| \gg |\rho_0\bar{v}\bar{w}|$. Interestingly, strong northward momentum fluxes ($\sim$0.1 N m^{-2} or 2 m^2 s^{-1}) are seen near 20 km in both June and August, decreasing to zero near 25 km. The resulting northward body forces are of the appropriate sign and magnitude to balance Coriolis torques on the westward zonal flow seen in Fig. 5 [cf. Eq. (4b)]. Given that the prevailing flow at 5-km altitude is from the northeast (Fig. 1), these observations are compatible with topographic gravity waves transporting northeastward momentum upward. The flux decreases to zero approaching the zero wind line near 25 km.

Above 30 km one finds a rapid upward increase in momentum transport from the west-northwest (Fig. 8). Strong convection occurred at this time in the Gulf of Panama and there is a good temporal agreement between subjective estimates of the daily convection in visible satellite images and the magnitude of these momentum fluxes one to two days later (Bywaters 1990). It is tempting to conclude that this is a manifestation of gravity-wave activity propagating from that remote source. The signal-to-noise ratio is fairly small above 30 km (Fig. 6), however, and the calculated body forces of $\sim$100 m s^{-1} day^{-1} cannot be readily balanced in Eq. (4). Reid and Vincent (1987) showed that insufficient temporal sampling, which in this case is less than 5 total hours above 32 km, can introduce errors. Therefore, we do not attach much significance to momentum fluxes above this level in the stratosphere.

b. Mesosphere

Mesospheric zonal (left) and meridional (right) momentum fluxes and body forces per unit mass for June and August are shown in Fig. 9. Since it is difficult

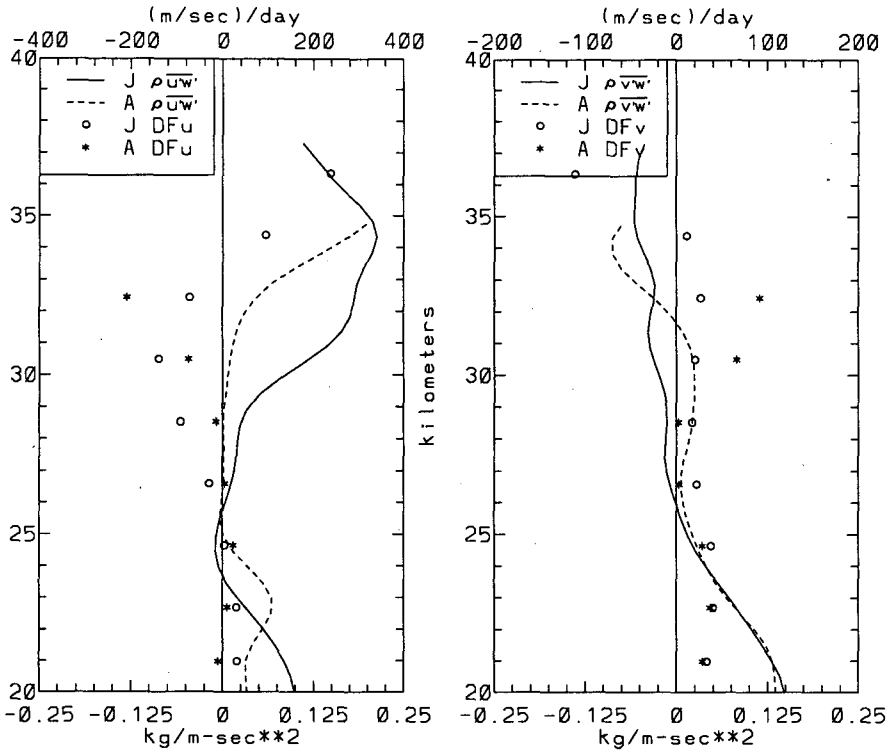

FIG. 8. Stratospheric profiles of zonal (left) and meridional (right) eddy momentum fluxes per unit volume (range $\pm$0.25 N m^{-2}) and corresponding body forces per unit mass (zonal range $\pm$400 m s^{-1} day^{-1}, meridional range $\pm$200 m s^{-1} day^{-1}), for the June (solid line and circles) and August (dashed line and asterisks) campaigns. The contribution by the time-mean circulation has been removed.

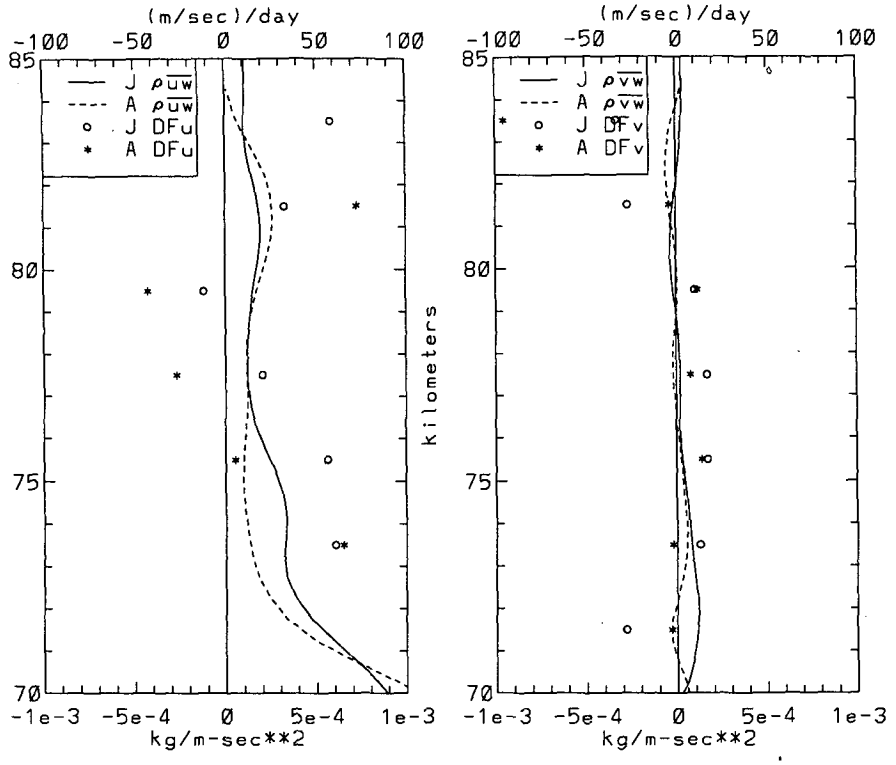

FIG. 9. Mesospheric profiles of zonal (left) and meridional (right) total momentum fluxes per unit volume (range $\pm 1 \times 10^{-3}$ N m^{-2}) and body forces per unit mass (range ± 100 m s^{-1} day^{-1}), for the June (solid line and circles) and August (dashed line and asterisks) campaigns.

to interpret mesospheric vertical motions we present the total fluxes and body forces, rather than the residuals. Zonal momentum fluxes in the 70–85-km region were $\sim 2 \times 10^{-4}$ N m^{-2} (or $\sim$2–8 m^2 s^{-2}), while meridional momentum fluxes were smaller, ~ 1 m^2 s^{-2}. Consistent with a filtering hypothesis, the fluxes generally opposed the flow (cf. Fig. 7). The zonal flow opposition is in agreement with the results of Vincent and Reid (1983) over Adelaide (35°S, 133°E) for the period 11–14 May 1981, although their magnitudes were $\sim$10 times smaller. Tsuda et al. (1989) reported that October 1986 mean values of $\overline{u'w'}$ in the 60–90-km layer at the Mu radar site (35°N, 136°E) were typically less than 1 m^2 s^{-2}. But during 9–17 June 1984, Fritts and Vincent (1987) found values of ~ -1 to -10 m^2 s^{-2} at Adelaide, and summer values at Poker Flat are typically $\sim$10–20 m^2 s^{-2} (Fritts and Yuan 1989). In all of these cases the sign of the flux opposed the flow and changed with the seasons. At Jicamarca below 78 km momentum fluxes were from the west-southwest during June and August, while the flow was from the east-northeast.

Body-force estimates are very sensitive to small vertical variations in momentum fluxes. Near 75 km DF_u was northeastward, compatible in sign with the observed wind changes from June to August (Fig. 7). These magnitudes of $\sim$10–100 m s^{-1} day^{-1} are comparable to Coriolis torques inferred from Jicamarca winds and to estimates at other sites (Fritts and Vincent 1987; Ruster and Reid 1990), residual budget estimates (Hitchman and Leovy 1988), and theory (Lindzen 1981; Holton 1983).

5. Discussion

The time-mean results of the 1987 Jicamarca campaigns revealed several interesting features of the tropical circulation that have not been detected with other measuring techniques. In the stratosphere strong local meridional circulations and momentum fluxes were found, together with a persistent layer of enhanced turbulence located $\sim$2 km above the descending eastward QBO maximum. The complex MSAO was documented for the boreal summer of 1987. Momentum flux and body-force estimates in the tropics were made for the first time. Despite this being a relatively new technique and despite possible systematic errors, the signs and magnitudes are compatible with Coriolis torques in the momentum equations. These results also contribute toward evidence of zonal variations of the flow at QBO levels and generally confirm expectations for this site located amid rich sources of topographic and convective gravity waves.

The classic theory of the QBO, due to Lindzen and Holton (1968), attributes the alternating layers of descending westerlies and easterlies to the absorption of vertically propagating Kelvin and mixed Rossby–gravity waves excited by tropical convection (Salby and

Garcia 1987). The planetary scale of these waves, together with the tendency to diagnose the QBO with monthly mean radiosonde data, encourages viewing the QBO as a zonal-mean phenomenon in the physical rather than in the statistical sense. During the last decade various investigators have suggested that gravity waves are also important in driving the QBO. Since these would be excited preferentially in regions of strong convection (Pfister et al. 1986) and topography, such as near Indonesia, South America, and Africa, the possibility arises that body forces due to gravity wave absorption would vary substantially in space. Quiroz and Miller (1967) showed that the onset of QBO easterlies in 1966 occurred more than one month later at Natal (6°S, 35°W) than at Ascension Island (8°S, 14°W). Large differences in zonal wind between Fort Sherman (9°N, 80°W) and Kwajalein (9°N, 168°E) were also reported by Hitchman et al. (1987), ranging from as much as 20 m s^{-1} in the lower stratosphere to 50 m s^{-1} in the mesosphere. Such variations may be attributed to the presence of gravity wave–driven regional circulations (Quiroz 1982, personal communication) or to extratropical planetary Rossby waves. At 10 m s^{-1} air would take about 40 days to travel around the equator, which would give considerable time for local momentum transfer to modify the flow. This may account for the stronger circulation near Jicamarca and the apparent preference for enhanced eastward flow near Indonesia. Klinker and Sardeshmukh (1992) have shown that parameterized orographic gravity waves in ECMWF forecasts lead to substantial zonal variations in the tropical stratosphere, and that the associated errors can be large. To the extent that gravity waves contribute to the zonal-mean QBO, it will be a challenge to estimate the net result of wave-driving events that vary a great deal in space and time.

Acknowledgments. We would like to thank Ron Woodman, director of the Jicamarca radio observatory, for many stimulating discussions, and the engineers who aided us in taking the data. We are grateful to Jose and Elio Loja, Barbara Naujokat, and Kevin Trenberth for kindly providing auxiliary data. We also thank Lenny Pfister and the reviewers for useful comments. We acknowledge support from NSF Grant ATM86-09507. MHH and KWB also acknowledge support from NASA Grants NAGW-1411 and NAG8-786 and NSF Grant ATM-8918574. EK and FS acknowledge support from NSF Grant ATM88-14629.

REFERENCES

Andrews, D. G., J. R. Holton, and C. B. Leovy, 1987: *Middle Atmosphere Dynamics.* Academic Press, 489 pp.

Avery, S. K., R. L. Obert, and J. P. Avery, 1989: Observations of equatorial mesospheric mean winds and tides. *Handbook for Middle Atmosphere Program,* SCOSTEP Secretariat, **28,** 64–67.

Balsley, B. B., and A. C. Riddle, 1984: Monthly mean values of the mesospheric wind field over Poker Flat, Alaska. *J. Atmos. Sci.,* **41,** 2368–2700.

Bywaters, K. W., 1990: Lower stratospheric gravity waves observed by the Jicamarca MST Radar, M.S. thesis, University of Wisconsin—Madison, 155 pp.

Coy, L., D. C. Fritts, and J. Weinstock, 1986: The Stokes drift due to vertically propagating internal gravity waves in a compressible atmosphere. *J. Atmos. Sci.,* **43,** 2636–2643.

Delisi, D. P., and T. J. Dunkerton, 1988: Seasonal variation of the semiannual oscillation. *J. Atmos. Sci.,* **45,** 2772–2787.

Dunkerton, T. J., 1982: Theory of the mesopause semiannual oscillation. *J. Atmos. Sci.,* **39,** 2681–2690.

——, 1985: A two-dimensional model of the quasi-biennial oscillation. *J. Atmos. Sci.,* **42,** 1151–1160.

——, 1991: Nonlinear propagation of zonal winds in an atmosphere with Newtonian cooling and equatorial wavedriving. *J. Atmos. Sci.,* **48,** 236–263.

——, and D. P. Delisi, 1985: Climatology of the equatorial lower stratosphere. *J. Atmos. Sci.,* **42,** 376–396.

Fritts, D. C., and R. A. Vincent, 1987: Mesospheric momentum flux studies at Adelaide, Australia: Observations and a gravity wave-tidal interaction model. *J. Atmos. Sci.,* **44,** 605–619.

——, and L. Yuan, 1989: Measurements of momentum fluxes near the summer mesopause at Poker Flat, Alaska. *J. Atmos. Sci.,* **46,** 2569–2579.

——, and D.-Y. Wang, 1990: Mesospheric momentum momentum fluxes observed by the MST radar at Poker Flat, Alaska. *J. Atmos. Sci.,* **47,** 1512–1521.

——, L. Yuan, M. H. Hitchman, L. Coy, E. Kudeki, and R. F. Woodman, 1992: Dynamics of the equatorial mesosphere observed using the Jicamarca MST radar during June and August 1987. *J. Atmos. Sci.,* **49,**

Garcia, R. R., and R. T. Clancy, 1990: Seasonal variation in equatorial mesospheric temperatures observed by SME. *J. Atmos. Sci.,* **47,** 1666–1673.

Gille, J. C., and L. V. Lyjak, 1986: Radiative heating and cooling rates in the middle atmosphere. *J. Atmos. Sci.,* **43,** 2215–2229.

Gray, L. J., and J. A. Pyle, 1989: A two-dimensional model of the quasi-biennial oscillation of ozone. *J. Atmos. Sci.,* **46,** 203–220.

Hamilton, K., 1982: Rocketsonde observations of the mesospheric semiannual oscillation at Kwajalein. *Atmos.-Ocean,* **20,** 281–286.

——, 1984: Mean wind evolution through the quasi-biennial cycle in the tropical lower stratosphere. *J. Atmos. Sci.,* **41,** 2113–2125.

——, and J. D. Mahlman, 1988: General circulation model simulation of the semi-annual oscillation of the tropical middle atmosphere. *J. Atmos. Sci.,* **45,** 3212–3235.

Hirota, I., 1978: Equatorial waves in the upper stratosphere and mesosphere in relation to the semiannual oscillation of the zonal wind. *J. Atmos. Sci.,* **35,** 714–722.

——, 1980: Observational evidence of the semiannual oscillation in the tropical middle atmosphere—A review. *Pure Appl. Geophys.,* **118,** 217–238.

Hitchman, M. H., and C. B. Leovy, 1986: Evolution of the zonal mean state in the equatorial middle atmosphere during October 1978–May 1979. *J. Atmos. Sci.,* **43,** 3159–3176.

——, and C. B. Leovy, 1988: Estimation of the Kelvin wave contribution to the semiannual oscillation. *J. Atmos. Sci.,* **45,** 1462–1475.

——, ——, J. C. Gille, and P. L. Bailey, 1987: Quasi-stationary, zonally asymmetric circulations in the equatorial middle atmosphere. *J. Atmos. Sci.,* **44,** 2219–2236.

——, J. C. Gille, C. D. Rodgers, and G. Brasseur, 1989: The separated polar winter stratopause: A gravity wave driven climatological feature. *J. Atmos. Sci.,* **46,** 410–422.

Hollingsworth, A., D. B. Shaw, P. Lonnberg, L. Illam, K. Arpe, and A. J. Simmons, 1986: Monitoring of observations and analysis quality by a data assimilation system. *Mon. Wea. Rev.,* **114,** 861–879.

Holton, J. R., 1975: *The Dynamic Meteorology of the Stratosphere and Mesosphere.* Amer. Meteor. Soc., 216 pp.

——, 1983: The influence of gravity wave breaking on the general

circulation of the middle atmosphere. *J. Atmos. Sci.*, **40,** 2497–2507.

Kiehl, J. T., S. Solomon, R. R. Garcia, and W. Grose, 1986: Tracer transport by the diabatic circulation deduced from satellite observations. *J. Atmos. Sci.*, **43,** 1603–1617.

Klinker, E., and P. D. Sardeshmukh, 1992: The diagnosis of mechanical dissipation in the atmosphere from large-scale balance requirements. *J. Atmos. Sci.*, **49,** 608–627.

Lindzen, R. S., 1981: Turbulence and stress owing to gravity waves and tidal breakdown. *J. Geophys. Res.*, **86,** 9707–9714.

——, and J. R. Holton, 1968: A theory of the quasi-biennial oscillation. *J. Atmos. Sci.*, **25,** 1095–1107.

Naujokat, B., 1986: An update of the observed quasi-biennial oscillation of the stratospheric winds over the tropics. *J. Atmos. Sci.*, **43,** 1873–1877.

Newell, R. E., and S. Gould-Steward, 1981: A stratospheric fountain? *J. Atmos. Sci.*, **38,** 2789–2796.

——, J. W. Kidson, D. G. Vincent, and G. J. Boer, 1974: *The General Circulation of the Tropical Atmosphere and Interactions with Extratropical Latitudes.* The MIT Press, 371 pp.

Oort, A. H., 1983: Global Atmospheric Circulation Statistics 1958–1973, NOAA Professional Paper 14. U.S. Dept. of Commerce, 180 pp.

Pfister, L., W. Starr, R. Craig, M. Loewenstein, and M. Legg, 1986: Small-scale motions observed by aircraft in the lower tropical stratosphere: Evidence for mixing and its relationship to large-scale flows. *J. Atmos. Sci.*, **43,** 3210–3225.

Plumb, R. A., 1984: The quasi-biennial oscillation. *Dynamics of the Middle Atmosphere,* J. R. Holton and T. Matsuno, Eds., Terra Scientific, 217–251.

——, and R. C. Bell, 1982: A model of the quasi-biennial oscillation on an equatorial beta-plane. *Quart. J. Roy. Meteor. Soc.*, **108,** 335–352.

Quiroz, R. S., and A. J. Miller, 1967: Note on the semiannual wind variation in the equatorial stratosphere. *Mon. Wea. Rev.*, **95,** 635–641.

Reid, I. M., and R. A. Vincent, 1987: Measurements of mesospheric gravity wave momentum fluxes and mean flow accelerations at Adelaide, Australia. *J. Atmos. Terr. Phys.*, **49,** 443–460.

Rood, R., A. Douglass, and C. Weaver, 1992: Tracer exchange between tropics and middle latitudes. *Geophys. Res. Lett.*, **19,** 805–808.

Ruster, R., and I. M. Reid, 1990: VHF radar observations of the dynamics of the summer polar mesopause region. *J. Geophys. Res.*, **95,** 10 005–10 022.

Salby, M. L., and R. R. Garcia, 1987: Transient response to localized episodic heating in the tropics. Part I: escitation and short-time near-field behavior. *J. Atmos. Sci.*, **43,** 458–498.

Trenberth, K. E., and J. G. Olson, 1988: An evaluation and intercomparison of global analyses from the National Meteorological Center and the European Centre for Medium-Range Weather Forecasts. *Bull. Amer. Metero. Soc.*, **69,** 1047–1057.

Trepte, C. R., and M. H. Hitchman, 1992: Tropical stratospheric circulation deduced from satellite aerosol data. *Nature,* **355,** 626–628.

Tsuda, T., S. Kato, T. Yokoi, T. Inoue, M. Yamamoto, T. E. VanZandt, S. Fukao, and T. Sato, 1989: Gravity waves in the mesosphere observed with the MU radar. *Handbook for Middle Atmosphere Program,* **28,** 257–260, SCOSTEP Secretariat.

Vincent, R. A., and I. M. Reid, 1983: HF Doppler measurements of mesospheric gravity wave momentum fluxes. *J. Atmos. Sci.*, **40,** 1321–1333.

——, and D. Lesicar, 1991: Dynamics of the equatorial mesosphere: First results with a new generation partial reflection radar. *Geophys. Res. Lett.*, **18,** 825–828.

Wehrbein, W. M., and C. Leovy, 1982: An accurate radiative heating and cooling algorithm for use in a dynamical model of the middle atmosphere. *J. Atmos. Sci.*, **39,** 1532–1544.

Woodman, R. F., and A. Guillen, 1974: Radar observations of winds and turbulence in the stratosphere and mesosphere. *J. Atmos. Sci.*, **31,** 493–505.

——, M. Leiva, and O. Castillo, 1989: New developments at the Jicamarca radio observatory. *Handbook for Middle Atmosphere Program,* **28,** 451, SCOSTEP. Secretariat.